Applied Surface Science 280 (2013) 33–41

Contents lists available at SciVerse ScienceDirect

Applied Surface Science

journal homepage: www.elsevier.com/locate/apsusc

Synthesis and characterization of nanostructured Mn(II) doped antimony-tin oxide (ATO) films on glass

Laxmikanta Dua [1], Prasanta K. Biswas *

Sol-Gel Division, CSIR-Central Glass and Ceramic Research Institute, 196 Raja S. C. Mullick Road, Kolkata 700032, India

ARTICLE INFO

Article history:
Received 9 August 2012
Received in revised form 3 March 2013
Accepted 17 April 2013
Available online 23 April 2013

Keywords:
Nanostructure
Ferromagnetism
Sol–gel
Excitons
Photoluminescence

ABSTRACT

Sol–gel Mn(II) doped antimony tin oxide films were developed with precursor of atomic ratio range, Sn:Sb:Mn = 68–72:23–25:9–3. The X-ray diffraction patterns depict tetragonal cassiterite phase of SnO_2. Transmission electron microscopy images suggest the nanostructured form of the doped materials. The increase in crystallite size with Mn(II) concentration is reflected by the larger band gap values (4.61–4.73 eV) arising from the excitonic transitions which also respond to PL emissions. Hall effect measurements show that the carrier concentration increases but mobility decreases for Mn(II) doping. Room temperature ferromagnetism with different saturation magnetic moments (M_s) has been observed for all dopant concentrations, 3–9 at%.

1. Introduction

SnO_2 film possesses the unique electrical, optical, electrochemical properties and high chemical stability. This is n-type electronic oxide and direct-band gap (3.87–4.3 eV [1,2]) semiconductor. This may have potential applications in the areas of liquid crystal display [3], gas sensing [4], ferroelectric transparent thin-film transistor [5], and windows for solar cells [6]. The structure of SnO_2 in its bulk form is usually tetragonal rutile/cassiterite with lattice parameters of $a = b = 4.737$ Å and $c = 3.186$ which is its only stable phase with space group of $P4_2/_{mnm}$ [7]. But polycrystalline or amorphous can also be observed in bulk as well as in thin film form which depends on the processing technique [8]. To obtain better electrical property, dopants including Sb, F, Mo etc. can be doped in SnO_2 matrix [9]. Among the doped SnO_2 TCO films, antimony doped tin oxide film (ATO) is a promising one as it shows better visible transparency and electrical conductivity. If the films are of nanoclusters then high degree of crystallinity without segregation occurs, which results in metal-like behaviour without grain boundary scattering despite of its high porosity [10]. Presently exhaustive work is being carried out on the nanostructured dilute magnetic semiconductors (DMS) in thin film form for their spintronic applications where optical, electrical and magnetic properties are operated simultaneously through a single material which also responds to photoluminescence property [11–13] for the dopant effect coupled with generation of nanoclusters leading to the formation of quantum dots. The dilute magnetic semiconductors are produced by doping with transition metal (TM) ions into non-magnetic semiconductors [14] to obtain carrier mediated magnetic property. As the nanostructured DMSs combine their electrical conductivity with ferromagnetism and optical transparency, they can be used in different multifunctional devices, such as spin-valve transistors, spin light-emitting diodes, non-volatile memories, ultra-fast optical switches, and so on [15]. Hence, several research groups have explored high temperature ferromagnetism in doped TiO_2, ZnO and SnO_2 semiconductors [16–22]. But, thrust has been given to the study of magnetic ion doped SnO_2 based DMSs as these covers ferromagnetism from low temperature to room temperature [20–23]. In addition, paramagnetic behaviour [24] cannot be ruled out in the above type DMS for the inhomogeneity in microstructure [25].

In addition, many theoretical studies on the possible magnetic behaviours of DMS materials have been done by different groups [26–31]. As for example, ferromagnetism did not exist in Co- and Mn-doped ZnO, unless additional p-type carriers were added which has been illustrated theoretically by Spaldin [27] through the local spin density approximation (LSDA). Jaffe et al. reported that oxygen vacancies played an important role in determining the magnetic properties of Co-doped TiO_2 [30]. Their results also exhibit that additional n-type carriers leading to increase in its density are required to stabilize the ferromagnetic state at relatively

* Corresponding author. Tel.: +91 33 2483 8082x3303; fax: +91 33 2473 0957.
E-mail addresses: pkbiswas@cgcri.res.in, prasantabiswascgcri@gmail.com, prasantabiswas2003@yahoo.com (P.K. Biswas).
[1] Present address: Salkia Hindu School (High & Unit-2), Salkia, Howrah 711106, West Bengal. India.

0169-4332/$ – see front matter © 2013 Published by Elsevier B.V.
http://dx.doi.org/10.1016/j.apsusc.2013.04.066

high temperature and accordingly Curie temperature increases [32,33]. Hence, it is clear that presence of free carrier in the DMS is essentially required. As Sb doped SnO_2 (ATO) is a n-type semiconductor, so it is expected that transition metal-ion-like Mn doping in the ATO system may develop room temperature ferromagnetism (RTFM) which may encounter bound magnetic polarons (BMP) as the material would possess magnetic cations, carriers and defects [34,35]. In addition to the above, band gap of bulk SnO_2 along with their charge carrier concentration, catalytic activity, the surface morphology, phase composition, crystallite size can be tailored by doping [36–38] with Gr(V) elements/TM which may be useful in electronics and photonics. Hence, in the present work, we are reporting the effect of manganese doping on the structural, electrical, optical along with quantum confinement and room temperature magnetic properties of antimony tin oxide (ATO) thin films prepared by the simplest sol–gel method.

2. Experimental

6 wt% equivalent SnO_2–Sb_2O_3–MnO precursor sols for Mn(II) doped antimony tin oxide films were prepared in alcoholic medium with the atomic ratio range, Sn:Sb:Mn = 67–72:23–25:3–9. The required amount of recrystallized hydrated stannic chloride (Loba Chemie, India, purity, 98%) was dissolved by a few ml of ethyl alcohol (dehydrated, Merck, Germany) and 1-propanol (for synthesis, E-Merck India Ltd.) solvent mixture (1:1, by volume) and stirred for 15 min. Similarly, required amount of antimony (III) chloride (purity ~98%, E-Merck, India Ltd.) was dissolved and stirred separately for 15 min in the same solvent mixture. After that another solution of Mn(II) acetate [$(CH_3COO)_2Mn, 4H_2O$] [purity ~98%, Alfa Aesar (a Johnson Matthey Co.)] with the same solvent mixture was prepared. Next, the antimony chloride solution and the manganese acetate solution were added separately to the tin chloride solution slowly while 2–3 drops of 10.5(M) HCl was added to the mixture in order to increase the solubility of antimony chloride preventing the precipitation of antimony oxychloride. The solution was stirred for 1 h and aged for 48 h for coating.

The films were developed onto Heraus make (Germany) Suprasil grade pure silica glass and also onto silica coated soda-lime silica glass by the dipping (Chemat 200, USA) technique in 10,000 class clean air room equipped with 100 class work station. The withdrawal speed was 4 cm/min. After each deposition the films was cured in air at 480 °C for 0.5 h. Thickness of the films was measured by Autogain L116B ellipsometer. Crystalline phase was identified by X-ray diffraction (XRD) pattern obtained from an X-ray diffractometer [Philips PW-1730 (Ni-filtered Cu K_α radiation)]. Micro structural study with the evaluation of nanocluster size of the Mn(II) doped ATO film was done by transmission electron microscopy (TEM) (Tecnai G^2 30.S – Twin, FEI company, Netherlands). Carbon coated 300 mesh Cu grid was used for TEM images. Elemental detection was done by EDS experiment utilizing the EDS set-up of transmission electron microscope. UV–VIS absorption and photoluminescence (PL) spectra were recorded using Shimadzu UV-VIS-NIR model (3101PC) spectrophotometer and Perkin Elmer fluorimeter (LS55) respectively. Hall mobility (μ), free electron carrier concentration (n_c) and resistivity (ρ) in a magnetic field of 0.51 T (Tesla) of the samples were measured at room temperature by HEM 2000 (EGK Corporation, Korea) using four-probe Van der Pauw method. The static magnetization (M) of thin films was measured as a function of static external field (H) by using a VSM (Model-7407) of Lakeshore Cryotronics.

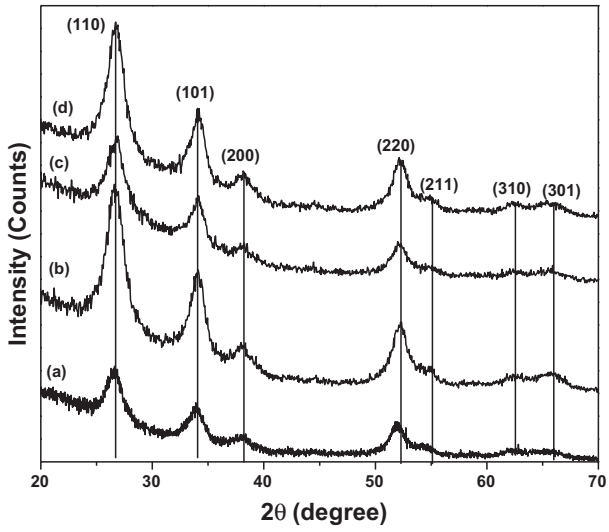

Fig. 1. X-ray diffraction pattern of the (a) 0 at%, (b) 3 at%, (c) 6 at%, (d) 9 at% Mn(II) doped antimony tin oxide (ATO) film.

3. Results and discussion

3.1. Structural analysis

The XRD study of the undoped and Mn(II) doped antimony tin oxide thin films deposited on glass substrates was done in the 2θ range of 20–70°. The cassiterite tetragonal SnO_2 phase was identified (JCPDS-77-0451) due to appearance of 2θ lines at 26.6°, 33.9°, 38.0°, 51.8°, 54.8°, 62.9° and 66.0° for the reflections from the planes (1 1 0), (1 0 1), (2 0 0), (2 1 1), (2 2 0), (3 1 0) and (3 0 1) respectively (Fig. 1). No characteristic phase of oxides of Sb(III)/Sb(V) and Mn(II) was observed. The reflection intensities from each XRD pattern can be related to the texture coefficient, $TC_{(hkl)}$ which can be calculated by using the equation (1) [39],

$$TC_{(hkl)} = \frac{I_{(hkl)}/I_{0(hkl)}}{(1/N)\sum I_{(hkl)}/I_{0(hkl)}} \quad (1)$$

where $I_{(hkl)}$ is the measured intensity of X-ray reflection, $I_{0(hkl)}$ is the corresponding standard intensity from the JCPDS data and N is the number of reflections observed in the XRD pattern. Fig. 2a depicts the variation in the texture coefficient with the at% of Mn(II) at different planes, (1 1 0), (1 0 1), and (2 0 0). It is interesting to note that texture of the ATO film can be increased if Mn(II) be doped. The texture coefficients are significantly high for the reflection from the plane (1 1 0).

The standard deviation (σ) of X-ray diffraction lines was estimated by using the following equation (2) to understand the growth mechanism involved in different doping levels of Mn(II) in antimony tin oxide (ATO) thin film.

$$\sigma = \sqrt{\frac{\sum I_{hkl}^2 - [(I_{hkl})^2/2]}{N}} \quad (2)$$

where I_{hkl} stands for the relative intensity of the (hkl) plane. The variation in standard deviation with the at% of Mn(II) is shown in Fig. 2b. It is seen that for undoped ATO film, the nucleation and adsorption–desorption phenomenon are predominant, which results in the heterogeneous nucleation because of relatively high σ values. A decrease in σ values with further increase in Mn(II) doping in ATO system suggests the onset of homogeneous nucleation.

Crystallite sizes (D) of the films were calculated using Scherrer's formula (Eq. (3)),

$$D = \frac{0.9\lambda}{\beta \cos \theta_{hkl}} \quad (3)$$

where θ_{hkl} is the Bragg angle that corresponds to the (hkl) lattice planes and λ is the wavelength of radiation (Cu K_α), and β is the